Nutrition
Research and
Practice

Original Research

Check for updates

Mentha canadensis attenuates adiposity and hepatic steatosis in high-fat diet-induced obese mice

Youngji Han [ID] [1], Ji-Young Choi [ID] [2], and Eun-Young Kwon [ID] [3,4,5§]

[1]Biological Clock-based Anti-aging Convergence Regional Leading Research Center of National Research Foundation of Korea, Korea University, Sejong 30019, Korea
[2]Department of Food and Nutrition, Chosun University, Gwangju 61452, Korea
[3]Department of Food Science and Nutrition, Kyungpook National University, Daegu 41566, Korea
[4]Center for Food and Nutritional Genomics Research, Kyungpook National University, Daegu 41566, Korea
[5]Center for Beautiful Aging, Kyungpook National University, Daegu 41566, Korea

OPEN ACCESS

§**Corresponding Author:**
Eun-Young Kwon
Department of Food Science and Nutrition, Kyungpook National University, 80 Daehak-ro, Buk-gu, Daegu 41566, Korea.
Tel. +82-53-950-6231
Fax. +82-53-950-6229
Email. eykwon@knu.ac.kr

ORCID iDs
Youngji Han [ID]
https://orcid.org/0000-0003-2270-8176
Ji-Young Choi [ID]
https://orcid.org/0000-0002-2022-3741
Eun-Young Kwon [ID]
https://orcid.org/0000-0001-8357-9158

ABSTRACT

BACKGROUND/OBJECTIVES: Obesity is a major risk factor for metabolic syndrome, a global public health problem. *Mentha canadensis* (MA), a traditional phytomedicine and dietary herb used for centuries, was the focus of this study to investigate its effects on obesity.
MATERIALS/METHODS: Thirty-five male C57BL/6J mice were randomly divided into 2 groups and fed either a normal diet (ND, n = 10) or a high-fat diet (HFD, n = 25) for 4 weeks to induce obesity. After the obesity induction period, the HFD-fed mice were randomly separated into 2 groups: one group continued to be fed HFD (n = 15, HFD group), while the other group was fed HFD with 1.5% (w/w) MA ethanol extract (n = 10, MA group) for 13 weeks.
RESULTS: The results showed that body and white adipose tissue (WAT) weights were significantly decreased in the MA-supplemented group compared to the HFD group. Additionally, MA supplementation enhanced energy expenditure, leading to improvements in plasma lipids, cytokines, hepatic steatosis, and fecal lipids. Furthermore, MA supplementation regulated lipid-metabolism-related enzyme activity and gene expression, thereby suppressing lipid accumulation in the WAT and liver.
CONCLUSIONS: These findings indicate that MA has the potential to improve diet-induced obesity and its associated complications, including adiposity, dyslipidemia, hepatic steatosis, and inflammation.

Keywords: Obesity; metabolic syndrome; herbal medicine; nonalcoholic fatty liver disease; diet, high-fat

INTRODUCTION

Obesity is a significant global health concern, and its prevalence has doubled worldwide since 1980. In 2009, the World Health Organization reported that over half a billion adults worldwide were overweight [1]. Obesity is a major contributing risk factor for various diseases, including dyslipidemia and hepatic steatosis [2]. Approved medications for obesity treatment often carry side effects and the potential for drug abuse [3]. While several anti-

obesity agents are effective for weight loss, many of them have limitations related to safety [4]. Throughout history, natural products derived from plants have been used as medicines and have proven to be a successful source of potential drugs. *Mentha canadensis* (MA), a plant species in the *Lamiaceae* family, is commonly known as an East Asian wild mint in Asia [5]. Compared to other mint species, it is particularly rich in natural menthol and pulegone, with menthol extensively used in various pharmaceutical preparations [6,7]. *Mentha piperita*, which belongs to the same genus as MA, is commonly used in Brazil for therapeutic purposes. Its usage has shown a reduction in body weight gain and improved lipid profiles in animals given juice extracted from its leaves [8]. However, no studies have investigated the anti-obesity effects of MA or elucidated its underlying mechanism. Therefore, the present study aimed to evaluate and characterize the molecular mechanism by which MA extracts exert anti-metabolic syndrome effects in diet-induced obese (DIO) mice.

MATERIALS AND METHODS

Sample preparation
MA was sourced from Puremind Co., Ltd. (Yeongcheon, Korea). The MA extract was obtained through an ultrasonic extraction process using 70% alcohol for more than 5 h, twice, at a temperature of 30°C (25 kW, 700–800 kHz). The resulting extract was filtered to remove any raw material residue, following the same method used for MA extraction. The MA extraction was then collected, concentrated, and freeze-dried. The yield of the extraction process was 33.72%. The dose of the MA alcohol extract was determined by previous studies [5,9].

Experimental animals and diet
Four-week-old male C57BL/6J mice (n = 35) were obtained from the Jackson Laboratory (Bar Harbor, ME, USA). Upon arrival, all mice were individually housed in the same room with a 12-h light-dark cycle at a controlled temperature of 22 ± 2°C. For the first week, they were fed a normal chow diet. Subsequently, the mice were randomly divided into 2 groups. One group (n = 10) continued to receive the normal chow diet (ND), while the other group (n = 25) was fed a high-fat diet (HFD) consisting of 60% of kilocalories from fat. This HFD feeding lasted for 4 weeks, aiming to induce obesity. After the obesity induction period at 9 weeks of age, the mice fed the HFD were randomly assigned to 2 groups. One group (n = 15) continued to receive the HFD alone (HFD group), while the other group (n = 10) received the HFD supplemented with 1.5% (w/w) MA ethanol extract (MA group) for a duration of 13 weeks (**Table 1**). Throughout the experimental period, all mice had free access to both food and distilled water. The body weight and food intake of all mice were regularly measured. All procedures conducted in this study were approved by the Animal Ethics Committee of Kyungpook National University (Approval No. 2017-0117).

Blood analysis
Plasma concentrations of total cholesterol (TC), high-density lipoprotein cholesterol (HDL-C), triglyceride (TG), and glucose were determined using commercial kits (Asan Pharm Co., Seoul, Korea). Plasma free fatty acid (FFA) concentration was determined using a commercial kit from Wako Chemicals (Osaka, Japan). Apolipoprotein (Apo) A-I and ApoB100 levels were measured using enzymatic kits (Eiken Chemical Co., Tokyo, Japan). NonHDL-C, HDL-C to TC (HTR), and atherogenic index (AI) were calculated as follows:

Table 1. Diet composition for animal experiment

Ingredient (g)	ND	HFD	MA
Casein	200	265	265
Corn starch	397.486	0	0
Sucrose	100	90	75
Dextrose	132	160	160
Cellulose	50	65.6	65.6
Soybean oil	70	30	30
Lard	0	310	310
Mineral mix[1]	35	48	48
Vitamin mix[2]	10	21	21
Calcium phosphate, dibasic	0	3.4	3.4
TBHQ, antioxidant	0.014	0	0
L-cystine	3	4	4
Choline bitartrate	2.5	3	3
MA			15
Total (g)	1,000	1,000	1,000
Total energy (kcal)	4,000	5,220	5,160

ND, normal diet (AIN-93G, 16% kcal from fat); HFD, high-fat diet (60% kcal from fat); MA, high-fat diet + *Mentha canadensis* ethanol extract (1.5%, w/w); TBHQ, tert-butylhydroquinone.

[1]AIN-93G-mineral mixture (g/kg): calcium carbonate anhydrous, 357; potassium phosphate monobasic, 196; potassium citrate tripotassium monohydrate, 70.78; sodium chloride, 74; potassium sulfate, 46.60; magnesium oxide, 24; ferric citrate, 6.06; zinc carbonate, 1.65; sodium meta-silicate·9H$_2$O, 1.45; manganous carbonate, 0.63; cupric carbonate, 0.30; chromium potassium sulfate·12H$_2$O, 0.275; boric acid, 0.0815; sodium fluoride, 0.635; nickel carbonate, 0.0318, lithium chloride, 0.0174, sodium selenite anhydrous, 0.01025; potassium iodate, 0.010; ammonium paramolybdate·4H$_2$O, 0.00795; ammonium vanadate 0.0066; powdered sucrose, 221.026.

[2]AIN-93G-vitamin mixture (g/kg): nicotinic acid, 3; Ca pantothenate, 1.6; pyridoxine-HCl, 0.7; thiamin-HCl, 0.6; riboflavin, 0.6; folic acid, 0.2; biotin, 0.02; vitamin B-12 (cyanocobalamin), 2.5; vitamin E (all-*rac*-α-tocopheryl acetate), 15; vitamin A (all-*trans*-retinyl palmitate), 0.8; vitamin D-3 (cholecalciferol), 0.25; vitamin K-1 (phylloquinone), 0.075; powdered sucrose, 974.655.

$$\text{NonHDL-C} = \text{TC} - \text{HDL-C}$$
$$\text{HTR (\%)} = (\text{HDL-C/TC}) \times 100$$
$$\text{AI} = (\text{TC} - \text{HDL-C})/\text{HDL-C}$$

Plasma levels of insulin, GIP, GLP-1, leptin, PAI-1, IFN-γ, IL-1β, IL-6, and IL-10 were measured using a MILLIPLEX kit (Merck Millipore, Billerica, MA, USA). All assays were performed according to the manufacturers' instructions.

Measures of hepatic and fecal lipid contents

Hepatic and fecal lipids were extracted following the method of Folch *et al.* [10]. Fecal samples from each group were collected daily for a week and subjected to lipid extraction. The dried hepatic lipid residues were dissolved in 1 mL of ethanol for subsequent analysis of TG, cholesterol, and FA. Emulsification of the dissolved lipid solution was achieved by adding Triton X-100 and a sodium cholate solution in distilled water to a final volume of 200 μL. Fecal samples were dried and extracted using an ice-cold mixture of chloroform and methanol (2:1 v/v) for 24 h at 4°C. After centrifugation at ×900 g for 10 min, the supernatant was collected, dried at 50°C, and dissolved in ethanol. The concentrations of hepatic and fecal TG, cholesterol, and FA were analyzed using the same enzymatic kits employed for the plasma analyses.

Activity measures of hepatic lipid-regulating enzymes

Hepatic mitochondrial, cytosolic, and microsomal fractions were prepared as previously described with slight modifications [11]. Protein concentrations were determined by Bradford method [12], and cytosolic fatty acid synthase (FAS) activity was measured by monitoring the malonyl coenzyme A (CoA)-dependent oxidation of NADPH at 340 nm [13]. Cytosolic malic enzyme activity was measured according to the method of Ochoa

et al. [14] by the production of cytosolic NADPH at 340 nm. Cytosolic G6PD activity was determined based on the reduction of 1 μmol of NADP per minute at 25°C, measured at 340 nm using a spectrophotometer, as described by Russo *et al.* [15]. Mitochondrial FA β-oxidation was measured by monitoring the reduction of NAD+ to NADH at 340 nm [16], while mitochondrial carnitine palmitoyl-CoA reductase activity was assayed following the method described by Markwell *et al.* [17]. Microsomal phosphatidate phosphatase activity was determined using a spectrophotometric method [18].

RNA isolation and gene expression analysis

All tissues were prepared and analyzed as previously described [19]. Total RNA was reverse transcribed to cDNA using the QuantiTect Reverse Transcription kit (Qiagen, Hilden, Germany). RNA expression was quantified by real-time quantitative polymerase chain reaction (PCR) using the QuantiTect SYBR Green PCR kit (Qiagen) and a SDS7000 sequence-detection system (Applied Biosystems, Foster City, CA, USA). Primers were designed to detect acetyl-CoA carboxylase (*Acc1*, 107476), CCAAT enhancer binding protein beta (*C/ebpb*, 12608), stearoyl-CoA desaturase 1 (*Scd1*, 20249), sterol regulatory element binding protein-1 (*Srebp1*, 20787), uncoupling protein 1(*Ucp1*, 22227), carnitine palmitoyltransferase 1 (*Cpt1*, 12894), peroxisome proliferator activated receptor alpha (*Ppara*, 19013), acetyl-CoA carboxylase beta (*Acc2*, 100705), peroxisome proliferative activated receptor, gamma, coactivator 1 alpha (*Pgc1a*, 19017), interleukin 6 (*Il6*, 16193), sirtuin 1 (*Sirt1*, 93759), tumor necrosis factor (*Tnfa*, 21926), tumor necrosis factor receptor superfamily, member 12a (*Tnfrsf12a*, 27279), tumor necrosis factor receptor superfamily, member 10b (*Tnfrsf10b*, 21933), 3-hydroxy-3-methylglutaryl-CoA reductase (*Hmgcr*, 15357), and acyl-CoA thioesterase 10 (*Acat*, 64833). Amplification was performed as follows: 95°C for 10 min, followed by 95°C for 15 s and 60°C for 60 s for 40 cycles. Cycle threshold values were normalized using glyceraldehyde-3-phosphate dehydrogenase (*Gapdh*). Relative gene expression was calculated using the $2^{-\Delta\Delta CT}$ method [20].

Morphology of liver and fat tissues

Liver and epididymal white adipose tissue (eWAT) were excised from the mice and immersed in a 10% formalin buffer solution for fixation. Subsequently, the fixed tissues were processed using standard procedures for paraffin embedding. Sections with a thickness of 4 μm were prepared and stained with hematoxylin and eosin as well as Masson's trichrome (MT). The stained sections were observed under an optical microscope (Nikon, Tokyo, Japan) at a magnification of 200×.

Energy expenditure (EE)

EE was measured using an Oxylet indirect calorimeter (Panlab, Cornella, Spain). The mice were individually placed in metabolic chambers at a temperature of 25°C, with ad libitum access to food and water. The oxygen (O_2) and carbon dioxide (CO_2) analyzers were calibrated using highly purified gas standards. Whole-body oxygen consumption (VO_2) and carbon dioxide production (VCO_2) were recorded at 3-min intervals using a computer-assisted data acquisition program (Chart 5.2; AD Instruments, Sydney, Australia) throughout a 24-h period. The data were averaged for each mouse. EE was calculated using the following equation:

$$EE (kcal/day/[kg \text{ of Body Weight} \times 0.75]) = VO_2 \times 1.44 \times [3.815 + (1.232 \times VO_2/VCO_2)]$$

Statistical analysis

Phenotype and microbiome data were expressed as the mean ± SE or SD. Statistical comparisons of HFD vs. ND and MA vs. HFD were performed by Mann-Whitney *U t*-test.

RESULTS

MA supplementation reduces body weight and body fat in mice

After a 4-week period of obesity induction, mice fed a HFD exhibited a significant increase in body weight compared to mice in the ND group, indicating DIO in the HFD group. However, dietary supplementation with MA resulted in a marked decrease in body weight and body weight gain, attributed to a reduction in food and energy intake (**Fig. 1A-C**). Furthermore, while there were no significant differences in the weights of subcutaneous and visceral white adipose tissue (WAT), the total WAT weight was significantly lower in the MA-treated group
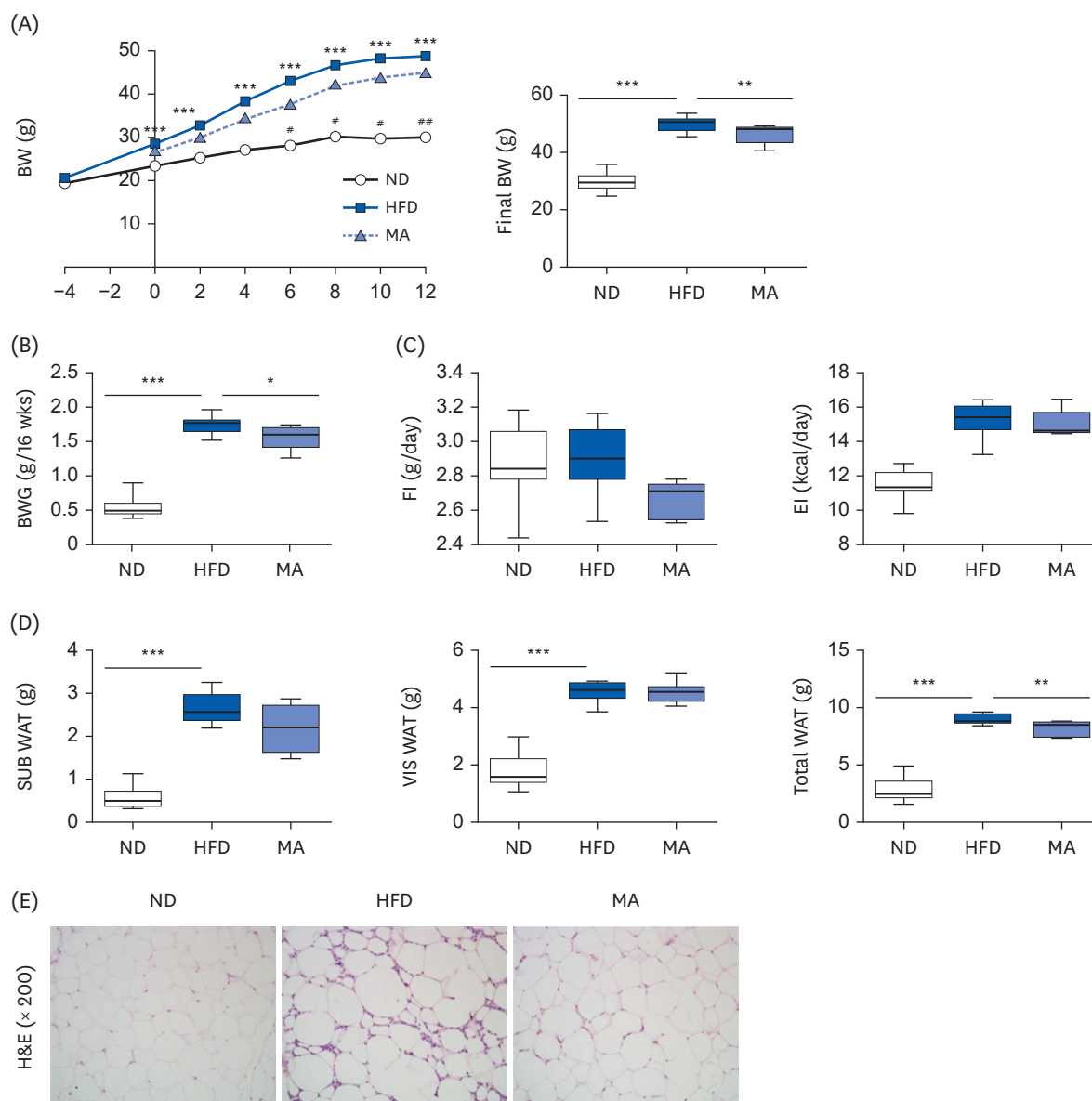

Fig. 1. Effects of 13-week *Mentha Canadensis* extract supplementation on body and adipocyte weights and eWAT morphology in C57BL/6J mice fed a HFD. (A) Changes in BW, (B) BWG, (C) FI and EI, (D) WAT weight, and (E) eWAT morphology. Data are presented as the mean ± SE. Representative eWAT photomicrographs shown at 200× magnification.
ND, normal diet; HFD, high-fat diet (20% fat and 1% cholesterol); MA, high-fat diet + *Mentha canadensis* ethanol extract (1.5%, w/w); H&E, hematoxylin and eosin-stained transverse section of epididymal white adipose tissue; eWAT, epididymal white adipose tissue; BW, body weight; BWG, body weight gain; FI, food intake; EI, energy intake; SUB, subcutaneous; VIS, visceral.
Mann Whitney *U* t-test; $^*P < 0.05$, $^{**}P < 0.01$, $^{***}P < 0.001$ vs. control.

compared to the HFD group (**Fig. 1D**). These findings were consistent with the observed morphology of eWAT (**Fig. 1E**).

MA supplementation increases EE and regulates associated gene expression of HFD mice

Hourly assessments of EE were conducted, and the results are presented in **Fig. 2A**. We observed a significant decrease in EE during the day compared to the nighttime measurements. However, in mice supplemented with MA, daytime EE was markedly higher compared to the HFD group. Immunohistochemical analysis of brown adipose tissue (BAT) revealed a significant increase in *Ucp1* expression and smaller BAT adipocyte size in the MA-supplemented group compared to the HFD group (**Fig. 2B**). Additionally, we analyzed the mRNA expression of 7 genes associated with lipid metabolism in eWAT (**Fig. 2C**) and found that MA supplementation significantly reduced the expression of *Acc1* and *Srebp1a*, while increasing the expression of *Ucp1* and *Ppara* compared to the HFD group.
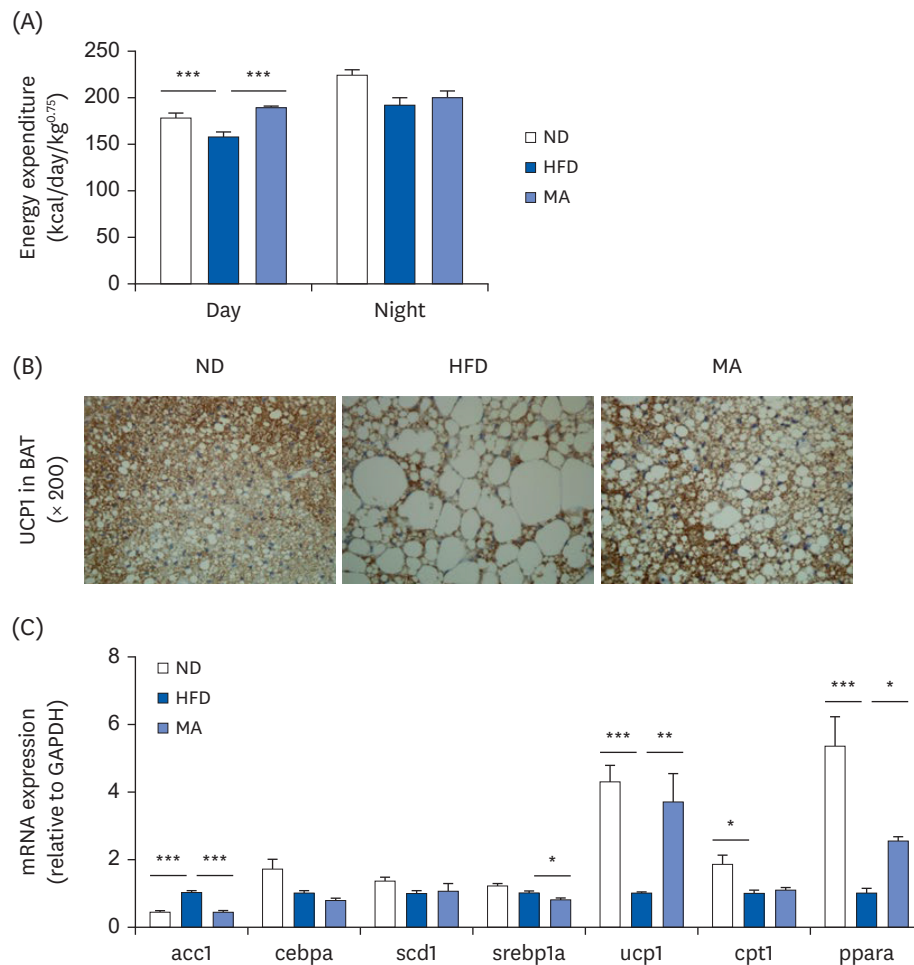

Fig. 2. Effects of 13-week *Mentha canadensis* extract supplementation on energy expenditure in C57BL/6J mice fed a HFD. (A) Measures of energy expenditure. (B) Immunohistochemistry of UCP1 staining in BAT (magnification 200×). (C) Measures of epididymal white adipose tissue mRNA expression of genes related to lipid metabolism. Data are presented as the mean ± SE.
ND, normal diet; HFD, high-fat diet (20% fat and 1% cholesterol); MA, high-fat diet + *Mentha canadensis* ethanol extract (1.5%, w/w); BAT, brown adipose tissue; GAPDH, glyceraldehyde-3-phosphate dehydrogenase.
Mann Whitney *U* *t*-test; $^*P < 0.05$, $^{**}P < 0.01$, $^{***}P < 0.001$ vs. control.

MA supplementation improves hepatic steatosis by altering enzymatic activity and gene expression of HFD mice

Furthermore, we observed that the HFD-induced increases in liver weight and hepatic lipid levels, including TG, cholesterol, and FFAs, were significantly attenuated by the administration of MA supplements (**Fig. 3A and C**). Additionally, the activities of FAS and malic enzyme were significantly reduced, while β-oxidation levels were significantly increased in mice from the MA group compared to the HFD group (**Fig. 3D**). Moreover, the mRNA expression of *Srebp1c*, *Fas*, and *Acat* was significantly decreased, whereas *Cpt1* expression was increased in the MA group compared to the HFD group (**Fig. 3E and F**). These results were consistent with our morphological observations, as evidenced by the reduced formation of lipid droplets in the liver tissue of mice in the MA group compared to those in the HFD group (**Fig. 3B**).

MA supplementation ameliorates plasma lipid profile and increases fecal lipid content of HFD mice

The plasma lipid profiles of our study groups are presented in **Fig. 4A**. We did not observe any significant differences in plasma levels of TG, FFA, and ApoB between the HFD and MA-supplemented groups. However, mice fed a HFD exhibited significant increases in plasma phospholipid (PL), TC, nonHDL-C, and ApoA-1 levels compared to those in the ND group. Interestingly, mice in the MA-supplemented group displayed lower values for these variables than those in the HFD group, along with an increase in fecal excretion of TG, FA, and cholesterol (**Fig. 4C**). Additionally, we observed a significant decrease in plasma leptin levels in the MA group compared to the HFD group (**Fig. 4B**).

MA supplementation ameliorates fibrosis and reduces cytokine secretion of HFD mice

Furthermore, we observed a significant decrease in plasma levels of inflammatory cytokines MCP1 and resistin in the MA group (**Fig. 5A**). MT staining of liver tissue and eWAT revealed the presence of fibrosis (blue color) in the HFD group, while no evidence of fibrosis was observed in mice from the ND or MA group. In fact, the tissue specimens from the MA group displayed a similar appearance to those from the ND group. Additionally, we found that hepatic mRNA expression of *Tnfrsf12a*, *Tnfrsf10b*, and *Sirt1* was significantly lower in the MA-supplemented group compared to the HFD group.

DISCUSSION

In the present study, we aimed to investigate the anti-obesity properties of MA and the potential mechanisms underlying its metabolic regulation in the context of an obesogenic diet. It is well known that when energy intake surpasses EE, it leads to an increase in body weight, with excess energy being stored as TGs in adipose tissue, ultimately resulting in overweight or obesity [21,22]. In our experimental design, mice were fed either a ND or a HFD to induce obesity over a 4-week period. The HFD-fed mice were then divided into 2 groups: the HFD group and the HFD with MA group. We observed that MA supplementation significantly suppressed body weight and reduced body fat during the experimental period, despite no changes in food and energy intakes. To support these findings, we also measured the metabolic rate, which showed a significant increase in EE in the MA group compared to the HFD group. In the process of adapting to protect the body from hypothermia, BAT, which is the best-known thermogenic system, expresses high levels of *Ucp1* to dissipate energy in the
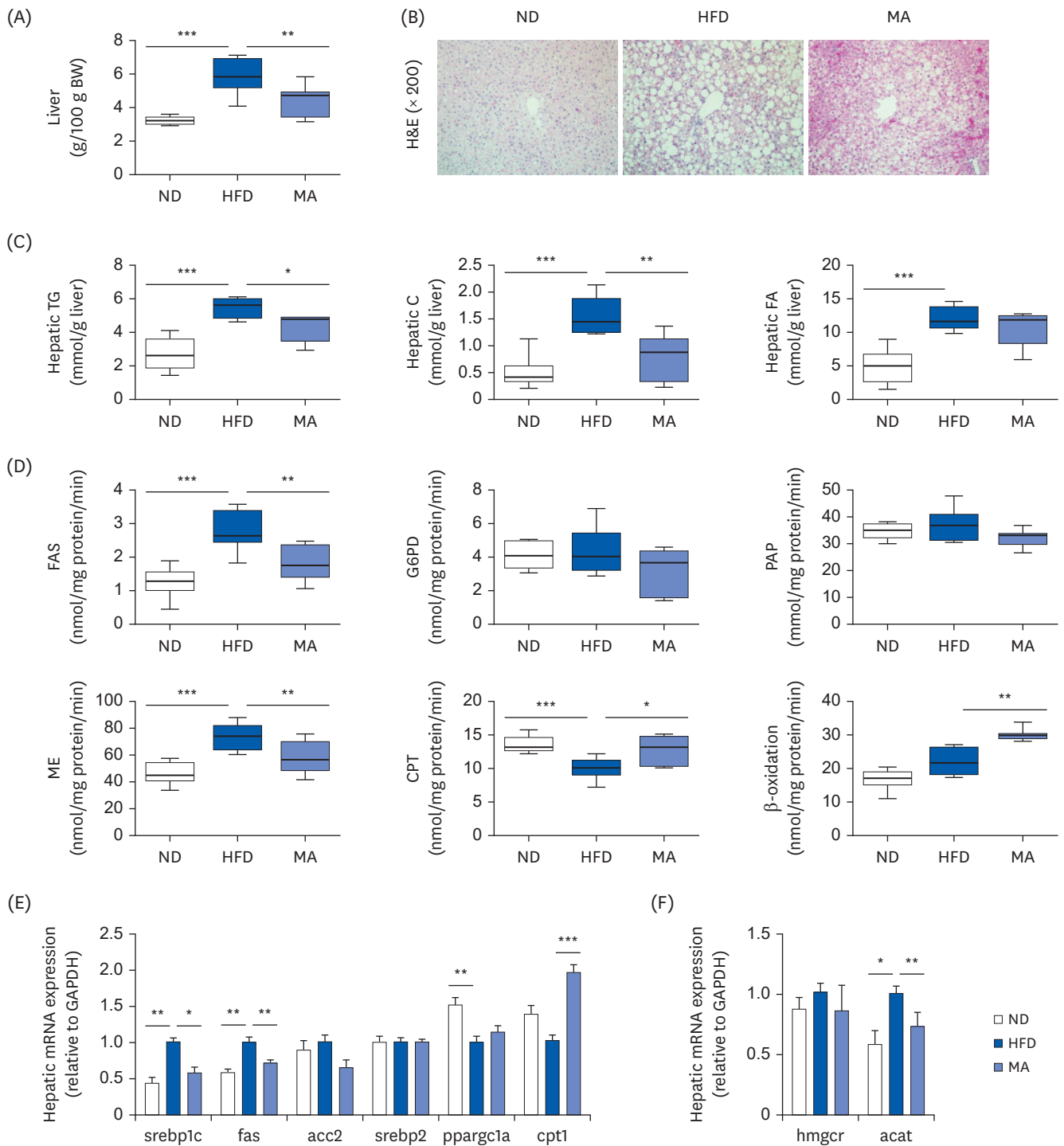
Fig. 3. Effects of 16-week *Mentha canadensis* supplementation on hepatic steatosis-related biomarkers in C57BL/6J mice fed a HFD. (A) Measures of liver weight. (B) Photomicrographs showing hepatic morphology (magnification 200×). Measures of (C) hepatic lipid contents and (D) hepatic enzyme activities related to lipid metabolism. (E, F) Hepatic mRNA expression levels of genes involved in lipid metabolism. Data are presented as the mean ± SE.
ND, normal diet; HFD, high-fat diet (20% fat and 1% cholesterol); MA, high-fat diet + *Mentha canadensis* ethanol extract (1.5%, w/w); FAS, fatty acid synthase, G6PD, glucose-6-phosphatedehydrogenase; PAP, phosphatidate phosphatase; ME, malic enzyme; CPT, carnitine palmitoyl-coenzyme A reductase; BW, body weight; TG, triglyceride; FA, fatty acid; FAS, fatty acid synthase; GAPDH, glyceraldehyde-3-phosphate dehydrogenase.
Mann Whitney *U* t-test; $^*P < 0.05$, $^{**}P < 0.01$, $^{***}P < 0.001$ vs. control.
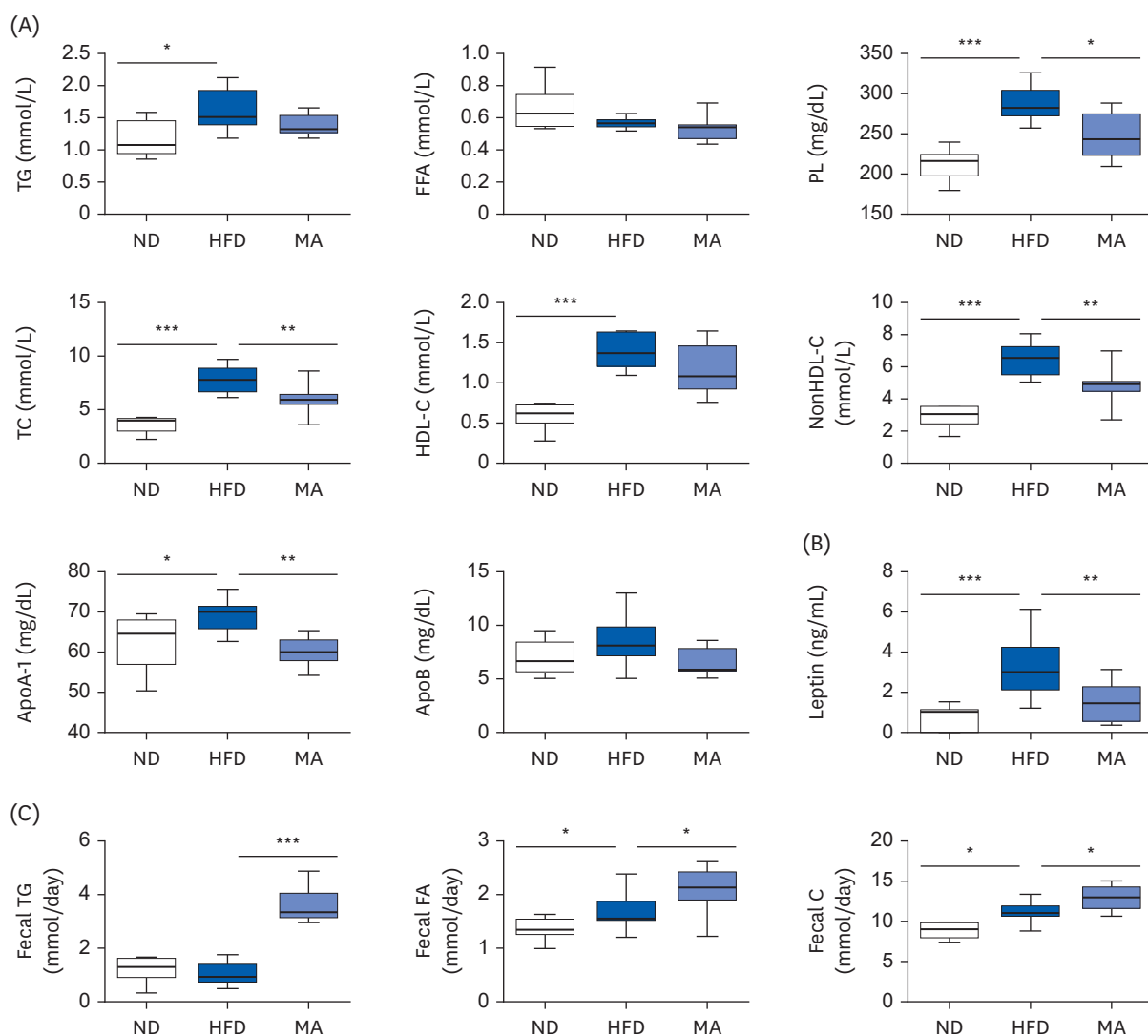
Fig. 4. Effects of 16-week *Mentha canadensis* supplementation on plasma and fecal lipid contents in C57BL/6J mice fed a HFD. (A) Plasma lipid profiles. (B) Plasma leptin levels. (C) Fecal lipid contents. Data are presented as the mean ± SE.
ND, normal diet; HFD, high-fat diet (20% fat and 1% cholesterol); MA, high-fat diet + *Mentha canadensis* ethanol extract (1.5%, w/w); TG, triglyceride; FFA, free fatty acid; PL, phospholipid; TC, total cholesterol; C, cholesterol; HDL, high-density lipoprotein; Apo, apolipoprotein.
Mann Whitney *U* t-test; *$P < 0.05$, **$P < 0.01$, ***$P < 0.001$ vs. control.

form of heat by uncoupling mitochondrial proton gradients during mitochondrial respiration [23]. *Ucp1* acts as a major regulator of adaptive thermogenesis, involving the uncoupling of oxidative phosphorylation from ATP synthesis by dissipating the proton gradient [24]. Similarly, EE is induced in response to excessive caloric intake, and animals with reduced thermogenic function are susceptible to DIO [25]. In our study, the MA supplementation significantly increased EE by inducing a notable upregulation of UCP1 expression in BAT, leading to a reduction in DIO. MA supplementation upregulated the expression of *Ucp1* in BAT and regulated the mRNA expression of genes related to lipid metabolism in eWAT.

The development of non-alcoholic fatty liver disease (NAFLD) is often associated with an increase in dietary lipids or adipocyte lipolysis, leading to elevated levels of FFAs [26]. Most obese individuals experience an increase in lipolysis from expanded fat cell mass, resulting in elevated FFA [27]. In the MA-supplemented group, we observed an elevation in lipogenesis
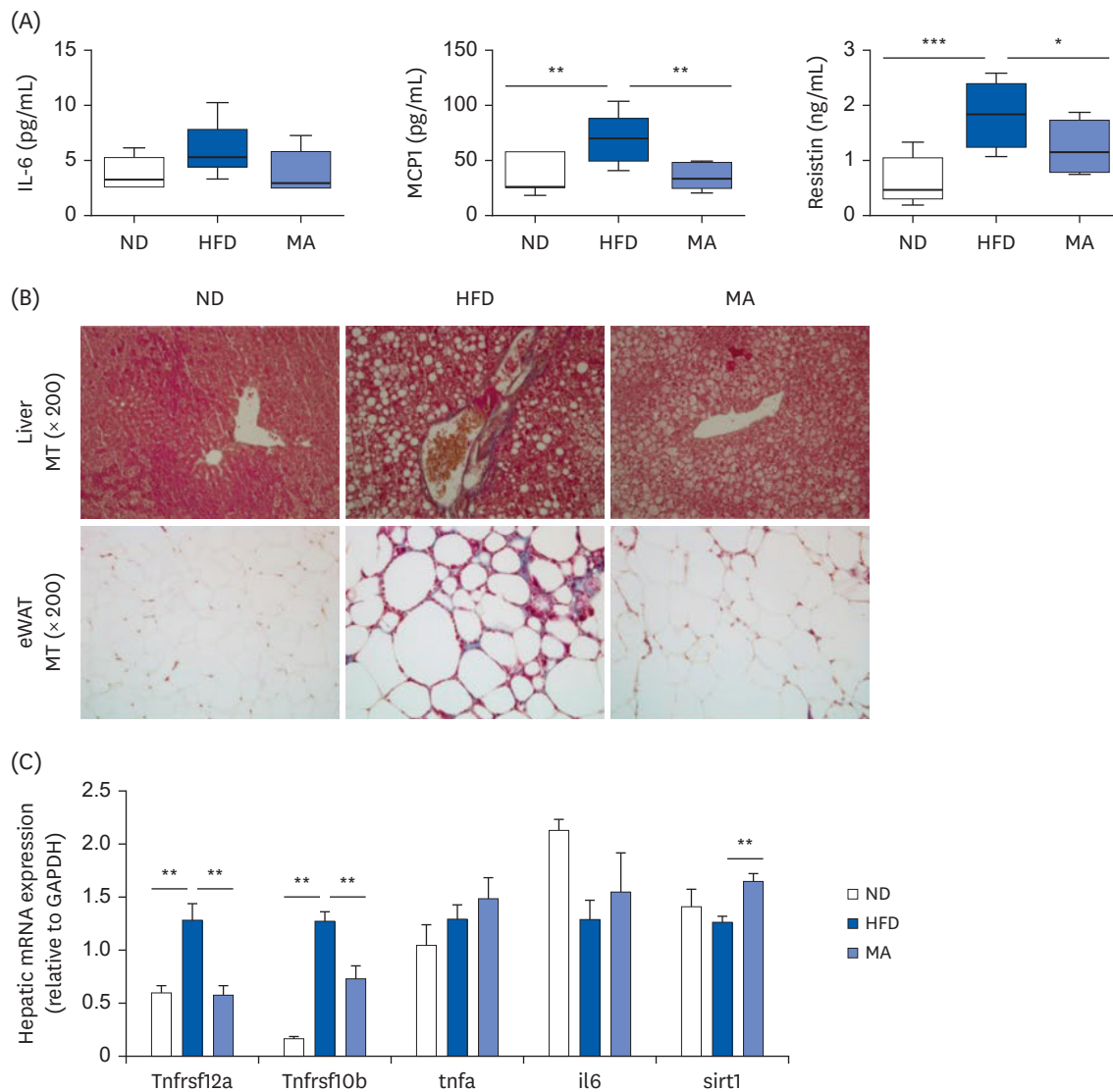
Fig. 5. Effects of 16-week *Mentha canadensis* supplementation on inflammation and fibrosis biomarkers in C57BL/6J mice fed a HFD. (A) Plasma cytokine levels. (B) MT staining of eWAT and hepatic tissue (magnification 200×). (C) Hepatic mRNA expression levels of inflammation-related genes. Data are presented as the mean ± SE.

ND, normal diet; HFD, high-fat diet (20% fat and 1% cholesterol); MA, high-fat diet + *Mentha canadensis* ethanol extract (1.5%, w/w); IL-6, interleukin 6; MCP1, monocyte chemoattractant protein-1; eWAT, epididymal white adipose tissue; MT, Masson's trichrome; GAPDH, glyceraldehyde-3-phosphate dehydrogenase. Mann Whitney *U t*-test; $^*P < 0.05$, $^{**}P < 0.01$, $^{***}P < 0.001$ vs. control.

through the upregulation of the FAS-related gene *Acc1* in eWAT, which helps prevent the transport of FFAs into the liver. The liver plays a crucial role in metabolic abnormalities, and the prevalence of metabolic syndrome and NAFLD is closely linked to obesity [28]. Dysregulation of lipid metabolism in the liver leads to abnormal accumulation of lipid droplets, known as hepatic steatosis [29]. MA supplementation increased *Srebp1-c* expression compared with HFD group, subsequently activating *Fas*, a transcription factor involved in FA and TG synthesis [30]. Additionally, MA supplementation upregulated the expression of the FA oxidation-related gene *Cpt1*. In the liver, FAs are converted to acyl-CoA, which is shuttled into mitochondria through *Cpt1* for β-oxidation. Acetyl-CoA, produced through glycolysis, is carboxylated by ACC2 to form malonyl-CoA, which inhibits *Cpt1* and the transfer of acyl-CoA for β-oxidation [31].

Our findings indicated a significant reduction in both liver weight and the size of lipid droplets in the liver. Similarly, hepatic lipid contents, including TG and cholesterol were decreased in mice of the MA-supplemented group. Moreover, MA supplementation increased the expression of hepatic *Ppargc1a* and *Cpt1*, while decreasing the expression of *Srebp1c* and *Acc2* compared to the HFD group. We also observed decreased levels of *Acat* and reduced hepatic cholesterol synthesis gene expression, as well as downregulation of malic enzyme activity in the MA group compared to the HFD group. Based on these findings, MA supplementation appears to exert a protective effect on liver disease, which normally progresses to fibrosis and cirrhosis, through the suppression of hepatic steatosis.

In our study, we also measured plasma markers including TC, PL, nonHDL-C, and ApoA levels. All these markers were decreased in the MA group. The reduction in HDL-C level in the MA-supplemented group can be attributed to a decrease in plasma TC concentration. Many sphingolipids and PLs have been implicated in obesity, insulin resistance, type-2 diabetes mellitus, and cardiovascular disease [15,31]. HFD significantly elevated plasma PL levels, whereas MA supplementation effectively lowered PL levels in mice. Therefore, MA supplementation may help prevent metabolic syndrome by suppressing body and liver weight and preventing dyslipidemia.

Adiposity is associated with the production and release of several inflammatory mediators, contributing to chronic low-grade inflammation [32,33]. Leptin, an adipokine primarily expressed in adipose tissue, plays a major role in the regulation of body weight [34]. Leptin can modulate the production of pro-inflammatory adipokines/cytokines. We found that MA supplementation significantly reduced plasma leptin levels and markedly decreased the levels of pro-inflammatory cytokines MCP1 and resistin. Additionally, the morphology of the liver and eWAT indicated an anti-fibrotic condition in the MA group, showing less advanced fibrosis. We also observed a significant decrease in the expression of inflammation-related genes (*Tnfrsf12a*, *Tnfrsf10b*, and *Sirt1*) in the liver and eWAT of the MA group compared to the HFD group. These results suggest that dietary MA treatment improves obesity-related inflammation, including reduced fibrosis in both eWAT and liver, by altering gene expression and plasma adipokine levels.

Our study has several limitations in the experimental design. The use of a single dosage of MA treatment prevents us from observing the concentration-dependent effects of MA extract. Furthermore, the absence of a positive control group results in insufficient evidence for the development of MA extract as an anti-obesity functional pharmaceutical material. We will perform the follow-up studies to verify the appropriate dosage in the near future. Additionally, we intend to establish a positive control group to secure the rationale for the development of MA extract as an anti-obesity functional pharmaceutical material

MA effectively suppresses body weight and increases daily EE. Further, MA improves hepatic steatosis by regulating the activities of lipid-metabolism-related enzymes and the expression of associated mRNA. Moreover, MA alleviates obesity-related inflammation by reducing cytokine secretion and modulating mRNA expression. These findings from our study demonstrate the potential of MA supplementation in effectively mitigating DIO and its associated complications.

REFERENCES

1. Bhurosy T, Jeewon R. Overweight and obesity epidemic in developing countries: a problem with diet, physical activity, or socioeconomic status? ScientificWorldJournal 2014;2014:964236.
   PUBMED | CROSSREF

2. Jung UJ, Choi MS. Obesity and its metabolic complications: the role of adipokines and the relationship between obesity, inflammation, insulin resistance, dyslipidemia and nonalcoholic fatty liver disease. Int J Mol Sci 2014;15:6184-223.
   PUBMED | CROSSREF

3. Fabbrini E, Sullivan S, Klein S. Obesity and nonalcoholic fatty liver disease: biochemical, metabolic, and clinical implications. Hepatology 2010;51:679-89.
   PUBMED | CROSSREF

4. Hasani-Ranjbar S, Nayebi N, Larijani B, Abdollahi M. A systematic review of the efficacy and safety of herbal medicines used in the treatment of obesity. World J Gastroenterol 2009;15:3073-85.
   PUBMED | CROSSREF

5. Tucker AO, Chambers HL. *Mentha canadensis* L. (Lamiaceae): a relict amphidiploid from the Lower Tertiary. Taxon 2002;51:703-18.
   CROSSREF

6. Hornok L. Cultivation and Processing of Medicinal Plants. Hoboken (NJ): Wiley; 1992.

7. Guenther E. The essential oils. New York (NY): D. Van Nostrand Company Inc.; 1961.

8. Barbalho SM, Spada AP, de Oliveira EP, Paiva-Filho ME, Martuchi KA, Leite NC, Deus RM, Sasaki V, Braganti LS, Oshiiwa M. Mentha piperita effects on Wistar rats plasma lipids. Braz Arch Biol Technol 2009;52:1137-43.
   CROSSREF

9. Yu X, Liang C, Chen J, Qi X, Liu Y, Li W. The effects of salinity stress on morphological characteristics, mineral nutrient accumulation and essential oil yield and composition in Mentha canadensis L. Sci Hortic (Amsterdam) 2015;197:579-83.
   CROSSREF

10. Folch J, Lees M, Sloane Stanley GH. A simple method for the isolation and purification of total lipides from animal tissues. J Biol Chem 1957;226:497-509.
    PUBMED | CROSSREF

11. Gesta S, Tseng YH, Kahn CR. Developmental origin of fat: tracking obesity to its source. Cell 2007;131:242-56.
    PUBMED | CROSSREF

12. Bradford MM. A rapid and sensitive method for the quantitation of microgram quantities of protein utilizing the principle of protein-dye binding. Anal Biochem 1976;72:248-54.
    PUBMED | CROSSREF

13. Nepokroeff CM, Lakshmanan M, Porter JW. [6] Fatty acid synthase from rat liver. Methods Enzymol 1975;35:37-44.
    CROSSREF

14. Ochoa S, Mehler AH, Kornberg A. Biosynthesis of dicarboxylic acids by carbon dioxide fixation; isolation and properties of an enzyme from pigeon liver catalyzing the reversible oxidative decarboxylation of 1-malic acid. J Biol Chem 1948;174:979-1000.
    PUBMED | CROSSREF

15. Russo SB, Ross JS, Cowart LA. Sphingolipids in obesity, type 2 diabetes, and metabolic disease. Handb Exp Pharmacol 2013;373-401.
    PUBMED | CROSSREF

16. Pitkänen E, Pitkänen O, Uotila L. Enzymatic determination of unbound D-mannose in serum. Eur J Clin Chem Clin Biochem 1997;35:761-6.
    PUBMED | CROSSREF

17. Markwell MA, McGroarty EJ, Bieber LL, Tolbert NE. The subcellular distribution of carnitine acyltransferases in mammalian liver and kidney. A new peroxisomal enzyme. J Biol Chem 1973;248:3426-32.
    PUBMED | CROSSREF

18. Walton PA, Possmayer F. The role of Mg2+-dependent phosphatidate phosphohydrolase in pulmonary glycerolipid biosynthesis. Biochim Biophys Acta 1984;796:364-72.
    PUBMED | CROSSREF

19. Han Y, Shin YC, Kim AH, Kwon EY, Choi MS. Evaluation of the dose-dependent effects of fermented mixed grain enzyme food on adiposity and its metabolic disorders in high-fat diet-induced obese mice. J Med Food 2021;24:873-82.
    PUBMED | CROSSREF

20. Livak KJ, Schmittgen TD. Analysis of relative gene expression data using real-time quantitative PCR and the $2^{-\Delta\Delta CT}$ method. Methods 2001;25:402-8.
    PUBMED | CROSSREF

21. Choi MS, Kim YJ, Kwon EY, Ryoo JY, Kim SR, Jung UJ. High-fat diet decreases energy expenditure and expression of genes controlling lipid metabolism, mitochondrial function and skeletal system development in the adipose tissue, along with increased expression of extracellular matrix remodelling- and inflammation-related genes. Br J Nutr 2015;113:867-77.
    PUBMED | CROSSREF

22. Hill JO, Wyatt HR, Peters JC. Energy balance and obesity. Circulation 2012;126:126-32.
    PUBMED | CROSSREF

23. Ikeda K, Yamada T. UCP1 dependent and independent thermogenesis in brown and beige adipocytes. Front Endocrinol (Lausanne) 2020;11:498.
    PUBMED | CROSSREF

24. Roesler A, Kazak L. UCP1-independent thermogenesis. Biochem J 2020;477:709-25.
    PUBMED | CROSSREF

25. Ono-Moore KD, Rutkowsky JM, Pearson NA, Williams DK, Grobe JL, Tolentino T, Lloyd KC, Adams SH. Coupling of energy intake and energy expenditure across a temperature spectrum: impact of diet-induced obesity in mice. Am J Physiol Endocrinol Metab 2020;319:E472-84.
    PUBMED | CROSSREF

26. Softic S, Cohen DE, Kahn CR. Role of dietary fructose and hepatic de novo lipogenesis in fatty liver disease. Dig Dis Sci 2016;61:1282-93.
    PUBMED | CROSSREF

27. Boden G. Role of fatty acids in the pathogenesis of insulin resistance and NIDDM. Diabetes 1997;46:3-10.
    PUBMED | CROSSREF

28. Yki-Järvinen H. Non-alcoholic fatty liver disease as a cause and a consequence of metabolic syndrome. Lancet Diabetes Endocrinol 2014;2:901-10.
    PUBMED | CROSSREF

29. Kwon EY, Jung UJ, Park T, Yun JW, Choi MS. Luteolin attenuates hepatic steatosis and insulin resistance through the interplay between the liver and adipose tissue in mice with diet-induced obesity. Diabetes 2015;64:1658-69.
    PUBMED | CROSSREF

30. Lauressergues E, Martin F, Helleboid A, Bouchaert E, Cussac D, Bordet R, Hum D, Luc G, Majd Z, Staels B, et al. Overweight induced by chronic risperidone exposure is correlated with overexpression of the SREBP-1c and FAS genes in mouse liver. Naunyn Schmiedebergs Arch Pharmacol 2011;383:423-36.
    PUBMED | CROSSREF

31. Wakil SJ, Abu-Elheiga LA. Fatty acid metabolism: target for metabolic syndrome. J Lipid Res 2009;50 Suppl:S138-43.
    PUBMED | CROSSREF

32. Monteiro R, Azevedo I. Chronic inflammation in obesity and the metabolic syndrome. Mediators Inflamm 2010;2010:289645.
    CROSSREF

33. Piya MK, McTernan PG, Kumar S. Adipokine inflammation and insulin resistance: the role of glucose, lipids and endotoxin. J Endocrinol 2013;216:T1-15.
    PUBMED | CROSSREF

34. Otero M, Lago R, Lago F, Casanueva FF, Dieguez C, Gómez-Reino JJ, Gualillo O. Leptin, from fat to inflammation: old questions and new insights. FEBS Lett 2005;579:295-301.
    PUBMED | CROSSREF